Design and Manufacturing the Torque Gauge of ICaSbot and Implementing its Data Transfer Protocol

M. H. Korayem*
Department of Mechanical Engineering,
University of Science and Technology, Tehran, Iran
E-mail: hkorayem@iust.ac.ir
*Corresponding author

A. Tajik
Department of Mechanical Engineering,
Science and Research Branch, Islamic Azad University, Tehran, Iran
E-mail: a.tajik@srbiau.ac.ir

H. Tourajizadeh
Department of Mechanical Engineering, IUST, Tehran, Iran
E-mail:hami1363@yahoo.com

Abstract: Sensors play a significant role in robotic fields. In this paper, a new approach is proposed to modify the measurement of cables' actual tension of a cable robot; furthermore, the unwanted noises of the constructed boards of the used sensors which amplify the loadcell output are reduced. Some applications are proposed for the mentioned measurement system. This approach has some advantages such as providing feedback for motors, evaluating the robot's ultimate load carrying capacity, improving the motor control system and estimating the vibrating deflections of the cables. Closed loop control of the robot and improvement of the robot's accuracy are some objectives of this work. In addition, a new approach is investigated in this paper to transfer data from loadcell to PC for a six Degree of Freedom (DOF) cable robot called ICaSbot. Flexible deflections of the cables' length are estimated using cable vibration theory for a specific path. The mechanism and its related designed boards are designed and manufactured. Besides, the output of the sensors is monitored and is used for calibrating the equations of the actual tension of the cables. The validity and efficiency of the proposed sensing device and its related claimed applications are proved by comparing the data of experimental tests with simulation results of MATLAB for two different predefined paths. The results show high accuracy of the measurement mechanism which can be used for online applications of the cable robots.

1   INTRODUCTION

To estimate the actual force of the cables and torque of the motors, in a cable robot, a proper and accurate cable tension measurement system is required. Feedback received from this measurement system can be used to have a better control of the robot. A proper torque measurement mechanism and its related accurate data transfer system are considered as the important and applicable components of a cable robot. Choosing correct mechanism to install on the robot, designing accurate data transfer system and gathering data from output of the loadcell which is used in this paper as the required torque measurement mechanism, allow us to obtain the actual cable tension and applied torque on the motors of a six-DOFs ICaSbot cable robot online and accurately during the robot motion.

One of the most applicable types of under constrained cable robots are cranes which are widely used in industry. This idea is related to cable-suspended robots; the researches have been started with the NIST RoboCrane in this field [1]. Evaluating the actual tension of the cables are desired for this type of robots while torque of the motors can be estimated through them which eventually leads to better torque control of the motors. Estimating the amount of flexibility of the cables and the maximum load carrying capacity of the robot are of other advantages of monitoring the actual tension of the cables. Previous researches on force sensors and torque measurement devices can be seen in [2-4]. In [5] a mechanism has been presented called "an experimental evaluation of human walking", where the authors have used cable-based measurement system in experimental test of human walking.

Ottaviano et al. have used torque measurement system in a 4-4 cable-based parallel manipulator for an application in hospital environment [6]. The type of the cable robot of IUST called "ICaSbot" is an under constrained cable suspended robot with six DOFs and six actuating cables supported by six motors [7-9]. In the prior researches, motors torque has been mostly estimated from its related angular velocity or has been obtained by the aid of strain gauges [10], [11]. To promote the performance of the robot into closed loop control and increase the accuracy of the system, measuring the actual tension of the cables is highly significant to be studied.

Considering the fact that the elasticity coefficient of the cables are low, the error appeared in the robot's trajectory and positioning of the robot is inevitable especially in the case that the robot carries a load on its end-effector. The tension of each cable in the robot movement had not been considered in the previous controlling attempts and this may lead to significant error in the robot positioning. Hence, to compute the actual tension of the cables, a new mechanism is proposed and designed in this paper using force sensors in order to close the control loop of the robot and evaluating its pay load capability and cables elasticity. The obtained results are compared with the simulation results of MATLAB. The second section describes the dynamic modeling of the cable robot and cables vibration theory, the third section describes the hardware setup which is employed in this research; the fourth section explains the designed GUI which is required for this setup. Force sensor calibration is discussed in the fifth section, and finally the efficiency of the proposed system is approved in the section six by conducting some experimental tests and analyzing and verifying them by the aid of simulation results.

2   FORMULATION

I. Dynamic Modelling

Regarding Fig. 1, for a spatial case of cable robot, assume a triangular shape end-effector which is suspended through six cables and has six degrees of freedom namely, $X = \{x, y, z, \varphi, \theta, \psi\}$, (three translational and three rotational). Using Newton–Euler equation leads to the following dynamics equation. It is proved that the tension of the cables may be described as below [12]:
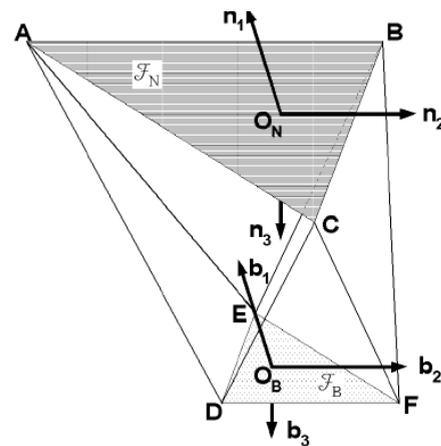

Fig. 1   Sketch of a cable system with its geometric parameters [13]

$$D(X)\ddot{X} + C(X, \dot{X})\dot{X} + g(X) = -S^T (q(X))T; \quad (1)$$

$$T = 1/r(\tau - J(d/dT(\partial\beta/\partial X)\dot{X} + \ddot{X}(\partial\beta/\partial X)) \\ -c(\partial\beta/\partial X)\dot{X}) \quad (2)$$

$$T = 1/r(\tau - J(d/dT(\partial\beta/\partial X)\dot{X} + \ddot{X}(\partial\beta/\partial X)) - c(\partial\beta/\partial X)\dot{X}) \quad (3)$$

$$D = \begin{bmatrix} mI_3 & 0 \\ 0 & P^T IP \end{bmatrix}; C = \begin{bmatrix} 0_3 \\ P^T \{ I\dot{P}\dot{o} + (P\dot{o}) \times I(Po) \} \end{bmatrix}; g = \begin{bmatrix} 0 \\ 0 \\ -mg \\ 0_3 \end{bmatrix};$$

$$S = \begin{bmatrix} q_i \\ x_j \end{bmatrix}_{i \times j}; P = \begin{bmatrix} 1 & 0 & -\sin\theta \\ 0 & \cos\psi & \sin\psi\cos\Theta \\ 0 & -\sin\psi & \cos\psi\cos\Theta \end{bmatrix}; \dot{o} = \begin{bmatrix} \dot{\Psi} \\ \dot{\Theta} \\ \dot{\phi} \end{bmatrix} \quad (4)$$

$$X = \{ x_m, y_m, z_m, \varphi, \theta, \psi \}$$

Where in Eq. (1), X is the vector of degrees of freedom of the system, $D(x)$ is the inertia matrix of the system, $C(x,\dot{x})$ is the Coriolis matrix, and $g(x)$ is the gravitational vector. In Eq. (2), $\tau(Nm)$ is the applied torque of motors, $J(kg.m^2)$ is the moment of inertia of the motors, $c(Nms/rad)$ is the viscosity coefficient of the motors, m is the mass of the end-effector, I is the moment of inertia of the end-effector, β is the angular velocity of the motors, r is the radius of the drum and q is the length of the cables. Finally I_3 is a unique diagonal matrix of size 3, 0_3 is a (3×1) zero vector, P^T is the transpose of matrix of P, T is the cables' tension and S is the Jacobian matrix of the system [2]. By the aid of this equation the required cables' tension can be calculated for controlling the end-effector on a predefined trajectory by the aid of inverse dynamics. The actual exerted tension can be then estimated using the proposed force sensor mechanism and the required improvements may be made.

II. Cable Tension Theory

As it can be seen from Fig. 1, in this model one end of the cable is connected to the motor of the robot and the other end is connected to the end-effector. The ith cable tension at the motor side and the end-effector end-side are U_i and f_i, respectively. According to the natural property of the cables which can be stretched but cannot be compressed, hence it is considered as $U_i \geq 0$ and $f_i \geq 0$. It may also be supposed that the cables' mass is negligible compared to the end-effector mass. The nominal length of the ith cable is L_i. It is also supposed that density, cross section area and cable Young modulus are constants. The vibrating equation of the cables may be explained as below [14]:

$$\frac{\partial^2 \omega_i(z_i,t)}{\partial z_i^2} = \frac{1}{c_i^2} \frac{\partial^2 \omega_i(z_i,t)}{\partial t^2} \quad (5)$$

$$\forall z_i \in (0, L_i), \ i = 1, ..., 6$$

where A_i is the cross section area of the cables, $\omega_i(z_i,t)$ is the vibrating deflection of the cable along its length (z_i), $C_i^2 = \frac{E_i}{\rho_i}$, E_i is the Young modulus of the cable and ρ_i is the constant density of the cables. The boundary conditions of the cable vibration may be explained as below:

$$E_i A_i \frac{\partial \omega_i(z_i,t)}{\partial z_i} \bigg|_{z_i=0} = u_i(t) \quad (6)$$

$$E_i A_i \frac{\partial \omega_i(z_i,t)}{\partial z_i} \bigg|_{z_i = L_i} = f_i(t) \quad ; i = 1, ..., 6$$

Where u_i is the tension of the upper side of the cable which is estimated using the proposed loadcell and $f_i(t)$ is the cable tension of the end-side which is connected to the end-effector and may be calculated using the control strategy. In this research, it is assumed that all cables are produced with same material and they have same cross section area; therefore, the Young modulus and cross sectional area are constant, so $A_i = A$, $C_i = C$ for $i = 1, ..., 6$. Based on the former assumption (neglecting the cable mass), u_i becomes constant for whole the cable length in Eq. (7) where:

$$EA \frac{\Delta \omega}{z} = u \quad (7)$$

By the aid of described methodology, the vibration deflection of the cables may be estimated using the mentioned force measurement system. The deflection of the cable may be obtained using Eq. (5). The Young Modulus of the cable is obtained equal to $2.08 \times 10^8 \ N/m^2$ for the employed cables by carrying out tension test on the cables. The cross sectional area of the cables is $4.9087 \times 10^{-6} \ m^2$ (the diameter of the used cable is equal to 2.5mm).

3   HARDWARE

I. Torque Measurement Mechanism

The torque measurement mechanism is designed in such a way that the force applied to the pulley could be transferred to the loadcell by the aid of a shaft. In the prior works the motors' torque were estimated from their rotational velocity and characteristics profile of the motor [15]. But by the aid of the new constructed mechanism, cable tension feedback can be evaluated accurately for any movements.

As it is shown in Fig. 2, the mechanism consists of three pulleys which are installed on the structure by means of three shafts. Two lateral pulleys are fixed and they only may rotate to transfer the cables while the central pulley not only is able to rotate but it may also move vertically up to 5 centimetres. This pulley is installed on the force sensor using some bolts. When two lateral pulleys transit the cables, the central pulley may move. The shaft connected to the force sensor can transfer the applied force to the sensor. The more the force, the greater is the pulley movement and the greater is the force sensor output.

Fig. 2   Loadcell used as the tension sensing device

Table 1   Specification of force sensor

Model	Single Point 1661
Material	Aluminum Alloy
Surface	anodized treatment
Size	$250 \times 350 \text{mm}^2$
Capacity	5kg
Excitation Voltage	$5 - 10 \text{Vdc}$
Output sensitivity	$2.0 \pm 0.1 \text{mv / v}$

The used force sensor (loadcell) is a single point aluminium alloy. As it is shown in Fig. 2 and Fig. 3 one side is connected to the pulley's shaft while the other side is connected to the upper platform of the robot by means of some bolts. This sensor consists of four strain gauges which convert the vertical applied force to voltage. Each resistance bridge (Fig. 4) including strain gauge excites the voltage up to $5 - 10 \, \text{V DC}$. The capacity of each sensor is up to $5 \, \text{Kg}$ and the accuracy is $0.1V + 0.2 \text{mV / V}$ [16]. Specification of each loadcell is listed in Table 1.
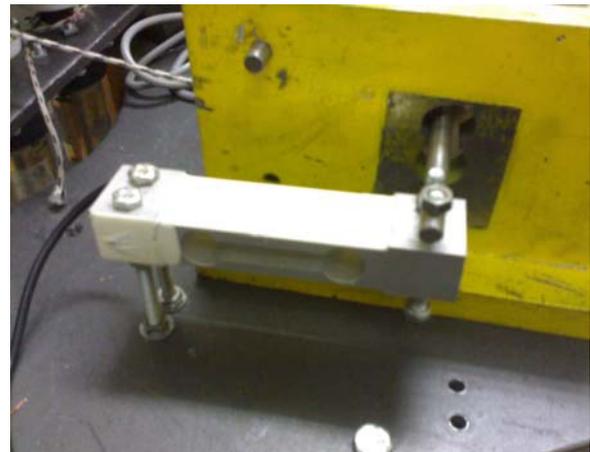

Fig. 3   Force sensor which is connected to the torque measurement mechanism

II. Data Transfer Protocol

Based on the proposed sensing device, a proper data transfer system is needed to handle the required data transfer process. Hence, an A/D sampling card is used. The output voltage of the loadcell is about $0.2 \, \text{mV}$. In order to measure this voltage, noise reduction and voltage amplification are unavoidable. To meet this goal an amplifier and noise reducer electronic board is constructed. This board consists of an amplifier IC (INA114) possessing a negative feedback in order to reduce the noises.

In addition to the negative feedback, INA114 has some advantages including: high signal to noise ratio (SNR), high and variable gain and low cost. The simplified schematic circuit of the electronic board is illustrated in the Fig. 4. 'U' and IC's of INA114, are used as amplifier and noise reducer, C's are the installed capacitors, J3 is the input voltage of the board, J1 and J2 are the output channels of the data card, and R1 to R6 are the resistance regulator for IC's. The mentioned electronic boards are simulated in Proteus software before manufacturing and acceptable results are obtained.
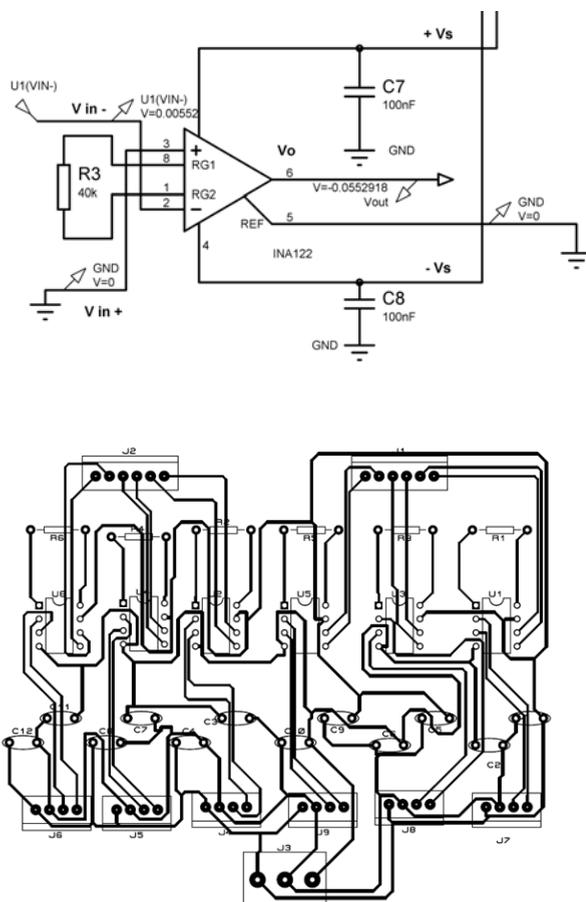
Fig. 4 Schematic circuit of the force sensor's output amplifier (Up) and circuit diagram of the PCB (Down)

boards in order to amplify the signals and decrease the noises and where they will be delivered to the data cards to be used in the program subsequently.

III. Robot Characteristics

The geometrical properties of the cable suspended robot in IUST (ICaSbot) are listed in Table 2, which is an under-constrained cable robot with six cables and six DOFs with a fix triangular shape platform and a moving triangular shape end-effector.

Table 2 Characteristics of the designed IUST cable robot

Body	
Height	120cm
Side length of base triangle	100 - 200cm
Weight	350kg
End effector	
Side length of base triangle	17cm
Thickness	8cm
Weight	1.100gr

Fig. 5 Scheme of the designed IUST cable robot

Eq. (8) and Eq. (9) calculate the INA114's output voltage and gain, respectively. The gain value depends on the R_G and it should be regulated from the excitation table from the INA114 datasheet [17]. V_O is the force sensor output voltage; V_{IN}^+ and V_{IN}^- are force sensor excitation voltages; and G is the force sensor amplification value which varies with variation of the resistance installed on the board.

$$V_O = G \times (V_{IN}^+ - V_{IN}^-) \tag{8}$$

$$G = 1 + \frac{50k\Omega}{R_G} \tag{9}$$

To control and record the data a 100 KHz analogue sampling card (Advantech PCI 1711L) is used which transfers force sensor output to PC. This card is an interface between the software and the amplifier board [18]. The output of the sensors are transferred to these

4 SOFTMARE

A GUI is designed for sending the required command and monitoring the recorded cables' tension. Using this software, robot may be controlled along different paths. Moreover, as it can be seen from Fig. 6 and Fig. 7, it is possible to record and observe the output of the sensor simultaneously in the designed control page of the GUI.
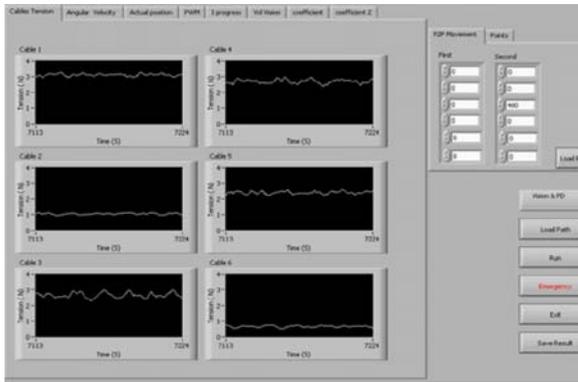
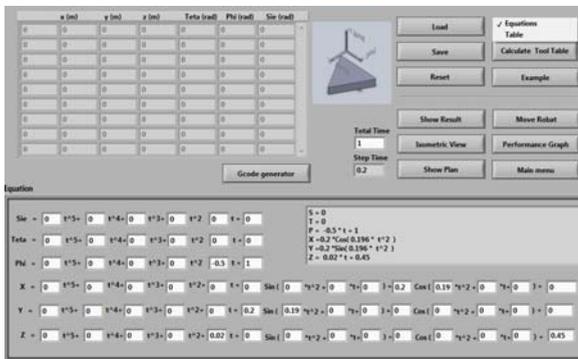**Fig. 6**　　A view of graphical environment to generate the robot path

Fig. 7　　Online display window of cable tension for each sensor output

5　FORCE SENSOR CALIBRATION

The force sensors are calibrated statically using several loads. Linear Eq. (10) may be used to calibrate each force sensor, where this equation is the relation between the cable tension and the force sensor output voltage. The calculated 'a' and 'b' coefficients of each sensor are listed in Table 3 [15]. In this equation, 'T' is the cable's tension (N); 'a' is the gain coefficient of the linear equation; 'b' is its offset and 'V' is the output voltage of the force sensor. 'a' and 'b' coefficients are extracted using static tests on each loadcell for two weights with different masses.

$$T = aV + b \tag{10}$$

$$T = Load(Kg) \times 9.81 \tag{11}$$

So the calibration is performed by the aid of a linear relation between the voltage and tension of Eq. (10) and the unknown variables are determined by the aid of some experimental tests as below:

Table 3　Coefficients of each sensor

Loadcell	a	b
1	3.85	-5.8935
2	6.5139	-1.9667
3	3.4234	-3.9662
4	2.8423	-1.4773
5	3.7574	-3.8498
6	5.4244	-0.226

6　COMPARISON OF SIMULATION RESULTS WITH EXPERIMENTAL RESULTS

In this section some experimental tests are conducted on the cable robot of ICaSbot and the obtained data are compared with the simulation results in order to show the validity of the mentioned experimental installation and the efficiency of the proposed applications. To meet this goal, two predefined trajectories which should be tracked by the robot are considered. For the first case, a right angled triangle trajectory should be traced by the end-effector. In this trajectory, end-effector starts from $x = 0, y = 10$, and $z = 0$. After tracking the mentioned triangle shown in Fig. 5, it stops at its first place after 7.5 seconds again. Output data of force sensors are monitored using Advantech 1711L sampling card every 0.2 seconds. The equation of this path is as follows:

$$Z = 0.9 \tag{12}$$

If t<2.5

X=0,Y=0.1−(0.1/2.5)×t

Else if 2.5<t<5

Y=0

X=(0.1/2.5)×(t-2.5)

Else

X=0.1−(0.1/2.5)×(t-5)

$Y = (0.1 / 2.5) \times (t-5)$

where 't' is time. Results from image processing obtained by camera and installed sensors on robot's end-effector are illustrated in Fig. 8. In this control approach, although the trajectory which is tracked by the robot has some deviations from its desired reference, it is obvious that controlling system has compensated it during the time. This acceptable compatibility confirms the correctness of the experimental setup. Slight deviations are related to un-modelled uncertainties. The cable tension results

obtained by installed loadcells on the robot and their related comparisons with simulation are also shown in Fig. 9 and Fig. 10.
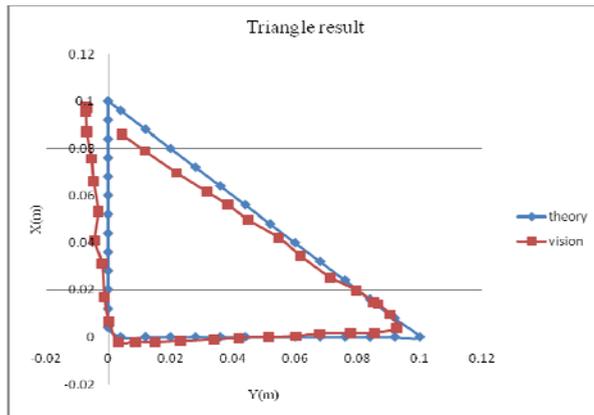

Fig. 8   Obtained results from image processing system for triangle motion
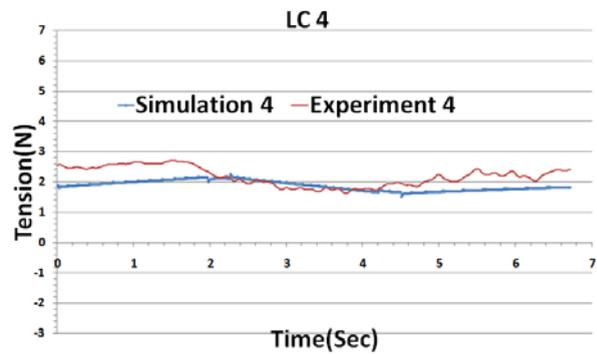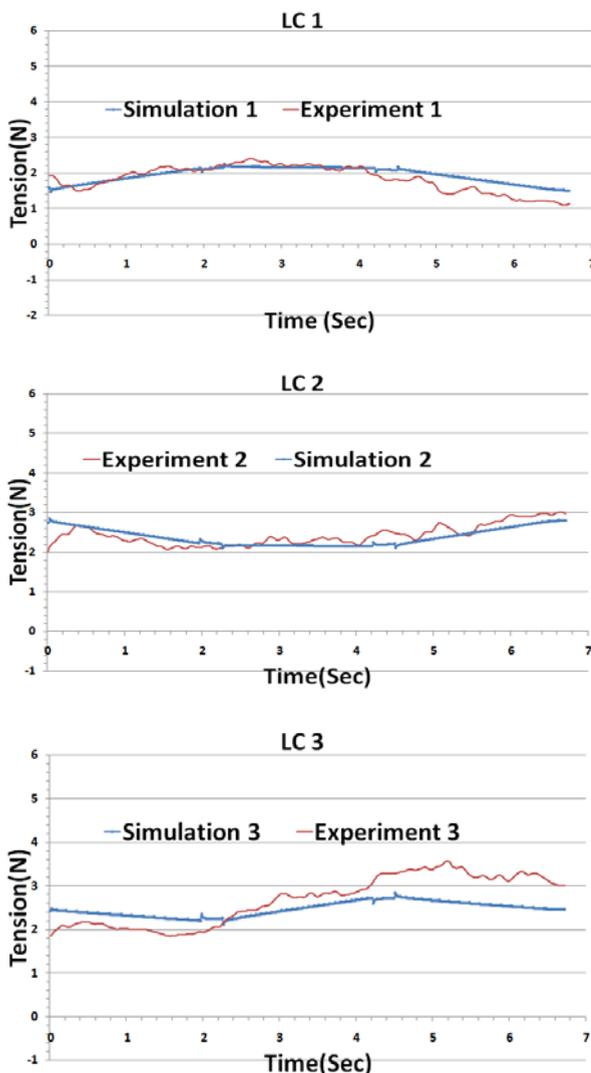

Fig. 9   Tension vs. Time - The first four results obtained by loadcells compared to simulation in a triangle trajectory. LC1) First loadcell output, LC2) Second loadcell output, LC3) Third loadcell output, LC4) Fourth loadcell output
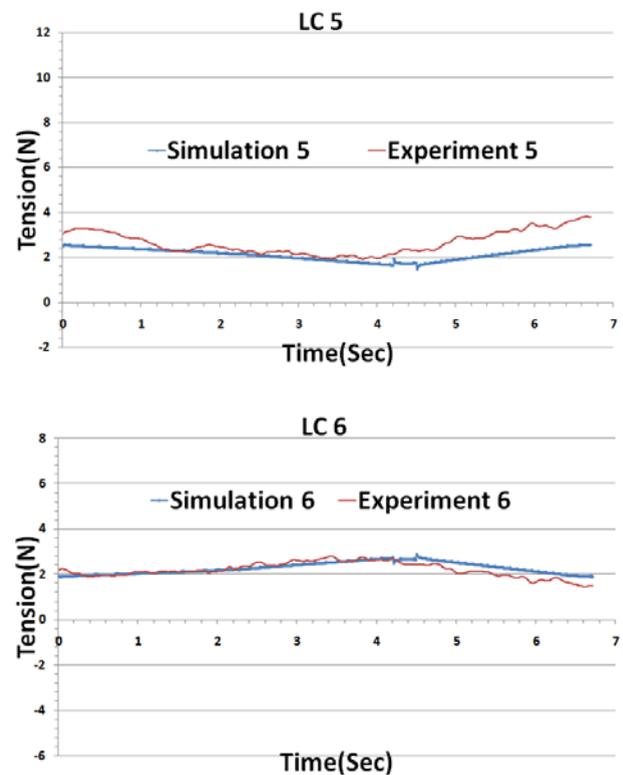

Fig. 10   Tension vs. Time - The two last results obtained by loadcells compared to simulation in a triangle trajectory. LC5) Fifth loadcell output, LC6) Sixth loadcell output

The blue lines in Fig. 9 and Fig. 10 are related to simulation results calculated by MATLAB while the red lines are the experimental results. As it is shown, although there are some differences in the beginning of the motion, however, the experimental results follow simulation results in the rest of the path which validates the efficiency of the proposed torque measurement mechanism.

It is worthwhile to note that, the differences are due to initial forces which apply to loadcells to overcome the friction and inertia of the motors. For the second path an inclined ISO circle trajectory is considered for the robot motion. To examine the capability of the robot to neutralize the destructive effect of the uncertainties, a 400 grams weight is placed on end-effector. The mentioned ISO trajectory follows as Eq. (13):

$$x = 0.05 \times \cos(2.685 \times \pi \times$$
$$(5.37 - t)^2 / 19.3568) \tag{13}$$

$$y = \cos(45 \times 2 \times \pi/360) \times (-0.05 \times \sin(2.685 \times \pi \times$$
$$(5.37-t)^2/19.3568))$$

$$z = \sin(45 \times 2 \times \pi/360) \times (-0.05 \times \sin(2.685 \times \pi \times$$
$$(5.37-t)^2/19.3568)) + \cos(45 \times 2 \times \pi/360) \times 0.8 + 0.3$$

The results obtained from the end-effector motion in x - y plane are depicted in Fig. 11, in which the results of two different controlling strategies including Cartesian space control (end-effector feedback) and joint space control (motor control) are compared with respect to the simulation results.
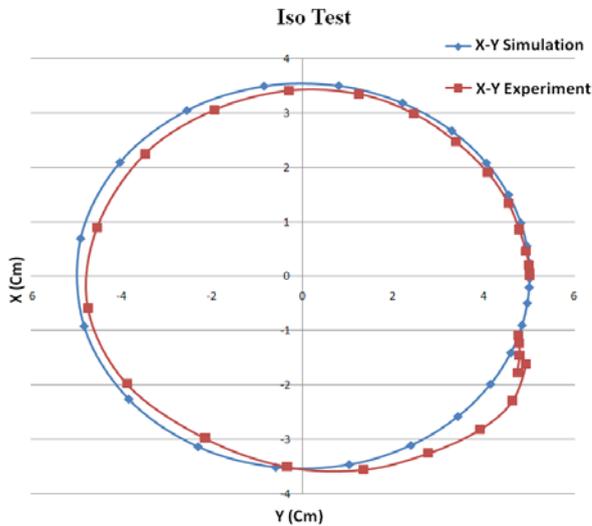

Fig. 11   Comparison of inclined circular trajectory between simulation and experiment

As it can be observed in Fig. 9, first of all the accuracy of the robot is higher in Cartesian space control approach during the motion tracking. Besides, there are some deviations at the beginning of the robot motion which are compensated during the trajectory by the aid of the controller. Moreover, since circular trajectory is traversed with height variation, the motion trajectory

appears elliptically in Fig. 11. The variation along z - axis is illustrated in Fig. 12.
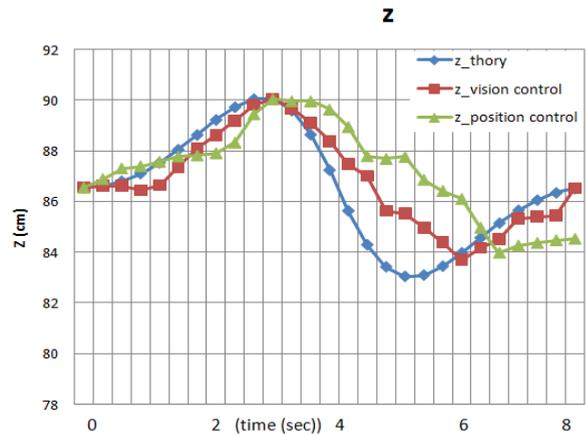

Fig. 12   Z-path of inclined circle

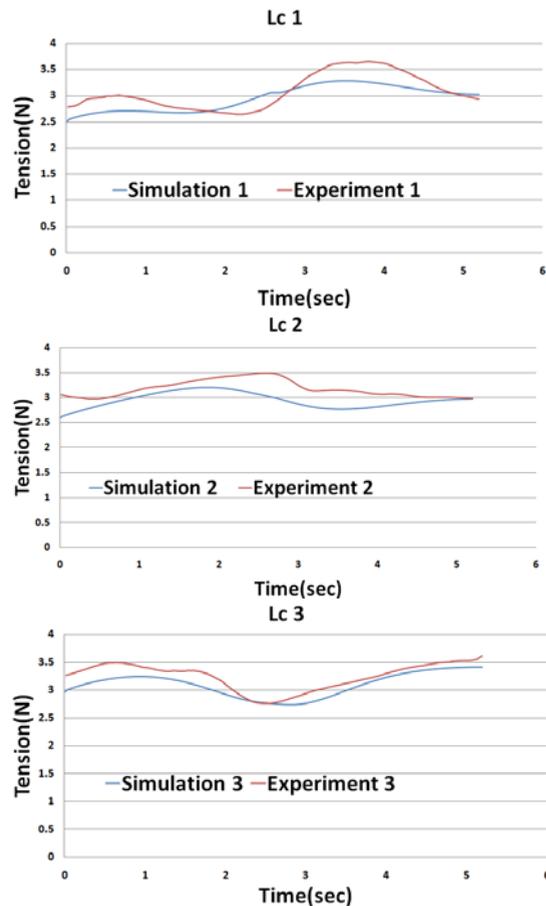Cables' tension are shown in Fig. 13 and Fig. 14.

Fig. 13   Tension vs. Time - The first three results obtained from force sensors for inclined circle with load. Lc1) First loadcell output, Lc2) Second loadcell output, Lc3) Third loadcell output
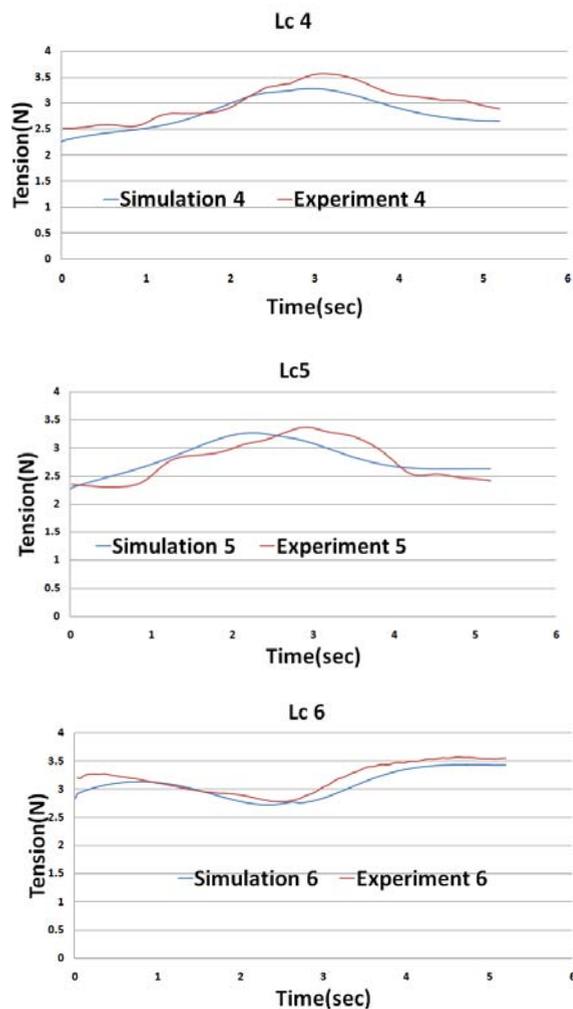
Fig. 14   Tension vs. Time - The second three results obtained from force sensors for inclined circle with load. Lc4) Fourth loadcell output, Lc5) Fifth loadcell output, Lc5) Sixth loadcell output

As it can be seen from diagrams, in some points cable tension value is deviated from simulation value which is due to the existence of excess load on end-effector and causes the experimental results to be higher than simulation values. Moreover, the deviations are compensated quickly by control system. It can be observed that the actual tension of the robot is usually higher than its related simulation results for the beginning moments of movement which is due to high applied forces on cables to overcome the un-modelled friction and inertia of the motors at the start stage of the movement.

Eventually, the compatibility of simulation and experiment is acceptable which validates the correctness of experimental tests. However, there are some oscillations in experimental diagrams compared to simulation which may be attributed to the following facts:

Because of using PD controller for the motors, the oscillation in the kinetic results of the robot is inevitable, where this oscillation may also have influences on the cable tensions. It should be noticed that, this oscillation is also observable in the angular speed diagram of the robot. In simulation diagram the longitudinal and transversal vibrations of the cables are not modelled. However the flexibility of the cables and also the structure of the robots practically affect the vibrating response of the robot. The used cables in this robot have high elastic characteristic and motion mechanisms from motors to end-effector have clearance especially in the joints, motors, drum, pulleys, flip flop, cable tension measuring mechanism, and cable conducting pulley, where these clearances highly affect the motion of the end-effector.

The vibration of the cables is also estimated by the aid of the installed loadcells using the formulation stated in section 2-2. While tracking a trajectory by the end-effector along vertical direction from $z = 100$ to $z = 80$ during 4 seconds motion with 0.02 second measurement accuracy, the cable length variation is shown in Fig. 15. Fig. 16 illustrates the Z variations with and without considering the cable vibrations. The output of the encoder for the motors is shown in Fig. 17.
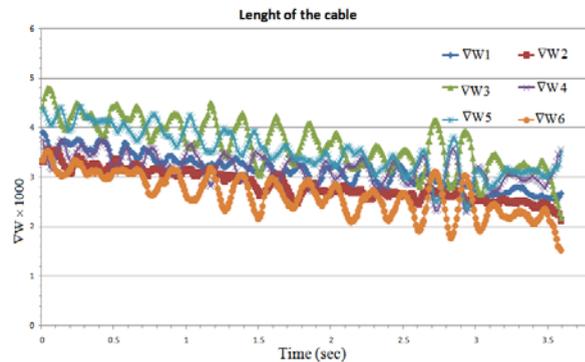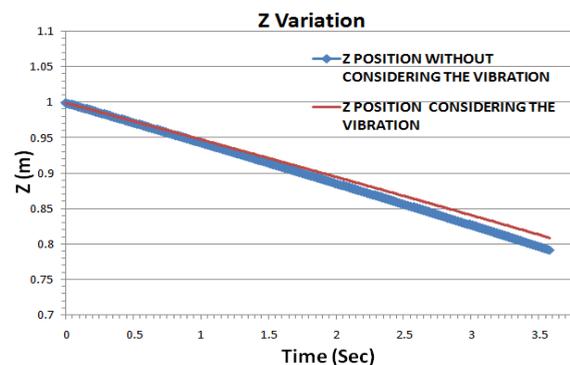

Fig. 15   Cable length variation

Fig. 16   Z variations with and without considering the cable vibrations
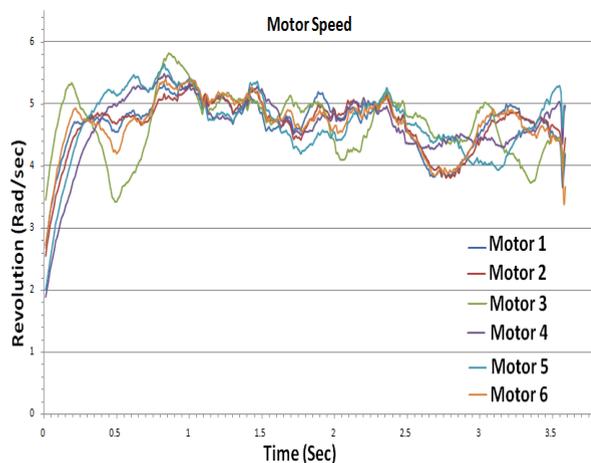
Fig. 17   Output of the encoder for motors

Two trajectories are compared in Fig. 16. The first trajectory is designed considering the cable vibration while this vibration is not considered in the second designed trajectory. The thick curve is related to trajectory which doesn't consider the cable vibration and the thin curve is related to trajectory considering the cable vibration. It can be seen that existence of flexibility of the cables affects the tracked motion of the end-effector in reality which is not observable in solid modelling of the robot. However, these little deviations which are in the order of 10^{-3} (based on the extracted profile of Fig. 15), are observable thanks to using the mentioned loadcell setup and employing the proposed vibration equations. The actual motion of the end-effector is plotted in Fig. 18.
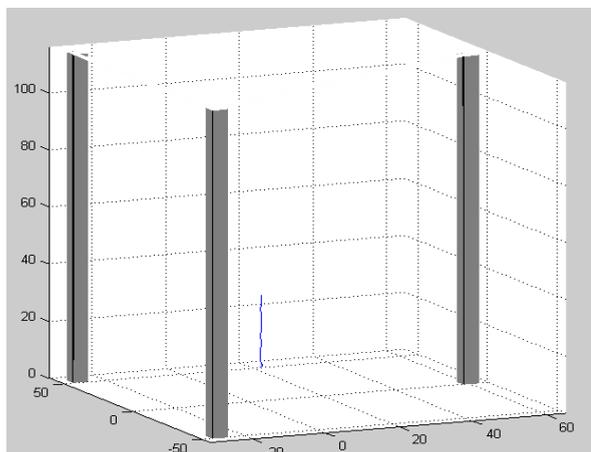

Fig. 18   Trajectory of the robot

8   CONCLUSION

A proper force sensor mechanism (i.e. loadcell) was

designed and implemented for ICaSbot cable robot to evaluate the actual tension of the cables of the robot during the movement. In order to achieve a smooth response without resonance, proper electrical boards were designed to amplify and filter the output data. Analog data card was used and installed to transfer the on-line data.

Moreover, a graphical user interface was provided to facilitate the required tests. A series of static tests were done with 0.2 second sample rate with different loads to calibrate the loadcells. The correctness of the calibration process was validated by the aid of comparing the tests with simulation results. It was seen that by means of the designed electrical boards and employed IC, the output noise of the sensor was decreased considerably and the accuracy of the output was increased.

Comparison of the experimental tests with simulation results has shown that not only an acceptable compatibility exist between simulation and experimental results which validates the correctness of the procedure, but there are also some vibrating behaviors of experimental signals around the mean value of simulation results which are due to clearance of the motor and joints, structural flexibility of the robot, cables vibration and etc.

Also it was observed that there is a difference between the value of cables tension at the initial moments of the movement between experiment and simulation which is the result of initial shock of the robot at the start moments of movement to overcome the static friction and inertia of the structure. However, this deviation is compensated by the aid of employed controller.

Furthermore, these differences are more severe in tests in which an additional weight is placed on the end-effector as an extra payload, since the cables' tension is increased during carrying this extra load.

It was stated that the proposed sensing device may help us to estimate the maximum load carrying capacity of the robot and evaluate the cables' vibration. It may also be used to have a more accurate motor control using the feedback of the torques. Moreover, the vibrating deflections of the cables which occur at the cables in reality and are not observable in solid modelling of the cables was evaluated by the aid of installed loadcells and proposed formulations.

It was observed that slight deviation in the order of 10^{-3} exists at the position of the end-effector as a result of the mentioned cable vibration which can be considered for more accurate controlling of the encoders. As a result, not only the actual cables' tension of the motors can be recorded in an online procedure by the proposed strategy, but also it may be used for some applications including evaluation of load carrying capability, torque control of the motors, and cables deflection estimation.

REFERENCES

[1] Albus, J., Bostelman, R., and Dagalakis, D., "The NIST ROBOCRANE", Journal Robot. Syst., Vol. 10, No. 5, 1993, pp. 709-724.

[2] Dwarakanath, T. A., Das Gupta, B., and Mruthyunjaya, T. S., "Design and development of a stewart platform based Force- torque sensor", Elsevier Journal Mechatronic, 2001.

[3] Briones, J. A., Castillo, E., Carbone, G., and Cecceralli, M,. "Position and force control of a parallel robot capaman 2 bis parallel robot for drilling tasks", Electronics, Robotics and Automotive Mechanics Conf., 2009.

[4] Kumar, V., and Keller, J., "Enabling feedback force control for cooperative towing robots", NSF Summer Undergraduate Fellowship in Sensor Technologies Clarence, Yale University, 2008.

[5] Ottaviano, E., Ceccarelli, M., and Grande, S., "An experimental evaluation of human walking", 3rd International Congress Design and Modelling of Mechanical Syst. CMSM'2009.

[6] Ottaviano, E., Ceccarelli, M., and Ciantis, M. D., "A 4-4 cable-based parallel manipulator for an application in hospital environment", Mediterranean Conf. on Control and Automation, Athens-Greece, 2007.

[7] Korayem, M. H., and Bamdad, M., "Dynamic Load Carrying Capacity of Cable-Suspended Parallel Manipulators", Int. Journal of Advanced Manufacturing Technology, Vol. 44, 2009, pp. 829-840.

[8] Korayem, M. H., Tourajizadeh, H., and Bamdad, M., "Dynamic Load Carrying Capacity of Flexible Cable Suspended Robot: Robust Feedback Linearization Control Approach", Journal of Intelligent Robot and Syst, Vol. 60, 2010, pp. 341-363.

[9] Korayem, M. H., Bamdad, M., and Saadat, M., "Workspace analysis of cable-suspended robots with elastic cable", in: IEEE International Conf. Robotics and Biomimetics ROBIO, 2007.

[10] Franitza, D., Torlo, M., Bekes, F., and Hiller, M., "Motion control of a tendon-based parallel manipulator using optimal tension distribution", IEEE/ASME Transactions on Mechatronics, Vol. 9, No. 3, September 2004.

[11] Nishibe, Y., Nonomura, Y., Tsukada, K., and Takeuchi, M., "Real time measurement of instantaneous torque by magnetostrictive sensor", IEEE Conf. on Digital Object Identifier, 1991.

[12] Alp, A. B., and Agrawal, S. K., "Cable suspended robots: design, planning and control", in Proc. Int. Conf. Robotics and Automation, Washington, DC, 2002, pp. 4275-4280.

[13] Alp, A. B., "Cable suspended parallel robots", Thesis for the Degree of Master of Science in Mechanical Engineering in University of Delaware, 2001.

[14] Pota, H. R., Agrawal, S. K., and Zhang, Y., "A flatness based approach to trajectory modification of residual motion of cable transporter systems", Journal of Vibration and Control, Vol. 10, No.10, 2004, pp. 1441-1457.

[15] Williams II, R., and Gallina, P., "Translational planar cable-direct-driven robots", Journal of Intelligent and robotic Syst., Vol. 37, 2003, pp. 69-96.

[16] Model 1661 Single Point Load Cells User Manual, BCM Sensor.

[17] BURR-BROWN Precision Instrumentation Amplifier, INA114 User Manual.

[18] Advantech Product, PCI1711L User Manual.